KEMENTERIAN
ALAM SEKITAR DAN AIR
Ministry of Environment and Water

MALAYSIAN METEOROLOGICAL DEPARTMENT
MINISTRY OF ENVIRONMENT AND WATER

Technical Note No. 2/2020

Coupling INSAT Multispectral Rainfall Algorithm (IMSRA) Using Thermal Infrared Channel from Himawari Satellite for Severe Rainfall Estimation in Malaysia

Noor Azam Shaari

TECHNICAL NOTE NO. 2/2020

Coupling INSAT Multispectral Rainfall Algorithm (IMSRA) Using Thermal Infrared Channel from Himawari Satellite for Severe Rainfall Estimation in Malaysia

By
Noor Azam Shaari

Contents

COUPLING INSAT MULTISPECTRAL RAINFALL ALGORITHM (IMSRA) USING THERMAL INFRARED CHANNEL FROM HIMAWARI SATELLITE FOR SEVERE RAINFALL ESTIMATION IN MALAYSIA

Noor Azam Shaari

Abstract

The rainfall distribution over certain locations may be affected due to the local weather system derived from nature. Extreme rainfall episodes over Malaysia have yet to be understood. Several rainfall estimation models that exist using the input parameter from the meteorological satellite are found to be promising to understand the phenomenon at a larger scale. The algorithm somehow requires an enormous effort to fine-tune, to match with the local weather and climate particularly for tropics. The established rainfall estimation model is expected to provide some valuable information for now-casting prior to the extreme rainfall hitting the region. The estimates from the rainfall estimation by INSAT Multispectral Rainfall Algorithm (IMSRA) using Brightness Temperature of Thermal Infrared (BT-TIR) as input parameters from both satellites INSAT-3D and Himawari were observed to be similar when compared with the actual satellite imagery. Higher correlation coefficient was observed to be about 0.9 between the estimates from both satellites. The correlation coefficient was observed to fall between 0.3 and 0.5 when compared between the estimates and ground observations. The correlation coefficient of the estimates was also evaluated between the ground observation with the other satellite-derived products of GPM-IMERG and GsMAP. The comparison of the correlation coefficient between ground observation and both satellite-derive products was best testified only at 0.5. Hence, a new algorithm to improve the severe rainfall estimation techniques for Malaysian region is essential to be established.

1.0 INTRODUCTION

Malaysia is located near an equatorial doldrums area where the climate characteristics are uniform in temperature, blessed with its high humidity and copious rainfall. The wind over the country is generally light and variable. Four weather seasons can easily be distinguished due to the changes in the wind flow and pattern. The prevailing wind flow is generally going southwesterly and easterly during the southwest and northeast monsoons, respectively. During the periods of strong surges of cold air from Siberia in the northeast monsoon, the prevailing wind may reach up to more than 30 knots and provide higher precipitation rates in the east coast of the peninsula. The main idea of the research is to understand the rainfall distribution over the Malaysian region. The rainfall distribution is measured using the estimation method from the techniques established by scientists from Indian Space Research Center (ISRO). The thermal infrared from Satellite Himawari at central wavelengths 10.4 $[\mu m]$ (Band 13) is applied as the parameters in the model for making estimation. Other than the model, the research is expected to establish and develop research skills and personal knowledge towards satellite meteorology applications particularly in rainfall estimation.

Extreme rainfall episode over tropics is a phenomenon that is still not well understood. The rainfall amount contributed during each rainfall event was not correctly captured and measured by any existing estimation models. Although several rainfall estimation models have been developed to understand the phenomenon, it still requires a significant amount of efforts to re-establish or fine-tune the algorithms to improve the accuracy.

2.0 OBJECTIVE

The weather and climate over maritime continental countries like Malaysia are often influenced by the complex interaction between the land and the ocean. The seasonal wind flow and topography commonly affects the rainfall distribution and intensity over the region. Severe flood is a common phenomenon during the

monsoon rainfall from November to January each year. Thus, this project is an effort to understand the phenomenon by improving the estimates in the study region. The estimates will undergo a certain validation process to quantify their accuracy. This is also an attempt to couple the existing rainfall estimation model by INSAT Multispectral Rainfall Algorithm (IMSRA) with the brightness temperature (BT) of Thermal Infrared (TIR) channel from the current operating satellite Himawari as the input parameters.

The aim of the project within the fellowship period is to observe the behavior of the estimates when the BT-TIR from different sensors and platforms are applied to the estimation model. The radiance over Malaysia and its neighboring countries is consistently measured by the Himawari geostationary satellite; hence, the availability of BT-TIR data from this satellite becomes an advantage to test the model's performance. The long-term goal from this is to produce its own rainfall estimation algorithm for observing instantaneous rainfall to support the current national disaster mitigation program by Malaysian Meteorological Department (MMD).

2.1 Scope of the study

The research conceived comprehensive studies from the past severe rainfall episodes that were inundated over the region, adopting theories, developing procedures and analyzing the accuracy. The estimates were analyzed and validated with in-situ observations and other satellite-derived rainfall products to statistically be compared and measured before choosing the best model that suits the region. The need to establish a new algorithm depends on how good are the results produced by IMSRA within this fellowship period. Since the new algorithm development requires a lot of time and effort, the work will continue in the home country. The establishment of the new algorithm is expected to be performed using the synergistic use of BT-TIR from satellite Himawari with the rainfall product of Dual-Frequency Precipitation Radar (DPR) by GPM.

2

The scope of the current research undertaken within the project scheduled includes these following steps:

- The rainfall estimation is carried out at both ocean and inland using BT-TIR of satellite Himawari and original BT-TIR from INSAT3D.
- The estimate is validated using in-situ observation and other satellite-derived products from GPM-IMERG and GSMaP.
- The result is fine-tuned using a correction method that has been developed by ISRO to match with local rainfall.
- Sets of procedures are performed to obtain the best result quantitatively and qualitatively.
- To learn basic ideas and methods to establish a new rainfall algorithm from the synergistic use of BT-TIR from satellite Himawari with the rainfall product of Dual-Frequency Precipitation Radar (DPR) by GPM. The work is expected to continue in the home country after the fellowship period.

3.0 DATA USED

3.1 Satellite Himawari

Himawari-9 was launched in 2017 as a backup-operation satellite of Himawari-8 that has been in orbit since 2015. Both satellites provide 13 observation bands and are scheduled to operate until around 2029. Each satellite carries Advanced Himawari Imager (AHI) scanning five areas: Full Disks, Japan Area (Region 1), the Target Area (Region 3) and two Landmark Areas (Region 4 and 5). In each 10-minute period, the AHI will scan Full Disks once, Japan Area and Target Area four times and the two Landmark Area twenty times. For the purpose of this research, the thermal infrared of the observation band 13 at central wavelengths 10.4 $[\mu m]$ is used. The dataset at higher spatial resolution of 0.05 degree in the NETCDF format is provided by Japan Aerospace Exploration Agency (JAXA) and downloaded from ftp://hokusai.eorc.jaxa.jp.

3.2 Satellite INSAT3D

Satellite INSAT-3D was developed by the Indian Space Research Organization (ISRO) and successfully launched on 26 July 2013 by using an Ariane 5 launch vehicle in the French Guiana. It is an advanced weather satellite configured with the improved Imaging System and Atmospheric Sounder. The development of this satellite seeks to enhance the meteorological observation and monitoring of land and ocean surfaces. The satellite carries four payloads of six channels of multispectral imagers, 19 channel sounders, Data Relay Transponder (DRT) and Search and Rescue Transponder. The Thermal Infrared (TIR) spectral channel at spatial and temporal resolutions of 4 km and 30 minutes' observation will be used as input parameters to the algorithm. For the purpose of this study, thermal IR or atmospheric window bands at wavelength 10.5 μm to 12.5 μm were applied in the algorithm (Gairola et al. 2015). The detail of the INSAT-3D data product is available from the Meteorological & Oceanographic Satellite Data Archival Center (MOSDAC) website at http://mosdac.gov.in.

3.3 GPM-IMERG

Integrated Multi-Satellite Retrievals for GPM (IMERG) is intended to inter-calibrate, merge, and interpolate "all" satellite microwave precipitation estimates, together with microwave-calibrated infrared (IR) satellite estimates, precipitation gauge analyses, and potentially other precipitation estimators at fine time and space scales for the TRMM and GPM eras over the entire globe. The system is run several times for each observation time, first giving a quick estimate and successively providing better estimates as more data arrive. The final step uses monthly gauge data to create research-level products (NASA-GPM ATBT, 2018). For the purpose of this study, the final product dataset at spatial resolution 0.1 degree is used and downloaded from the official website at ftp://arthurhou.pps.eosdid.nasa.gov.

3.4 GPM-DPR

The Global Precipitation Measurement (GPM) Core Observatory spacecraft is an advanced successor to TRMM with an additional channel on both Dual-frequency Precipitation Radar (DPR) and GPM Microwave Imager (GMI). Both channels have the capabilities to observe light rain and falling snow (Hou et al. 2014, Hou et al. 2008). The spacecraft was launched in February 2014 and it currently operates in a non-sun synchronous orbit at the inclination angle of 65 degrees. The precipitation from the tropics to the Artic and Antartic circles is observed at all hours. The DPR with Ku-band (35.5 GHz) and Ka-band (13.6 GHz) channels provides a three-dimensional (3D) precipitation (rain and snow) particle structure with a vertical resolution of 250m, a horizontal resolution of ~5 km, and a swath width of 125 km (Ka) and 245km (Ku) (Hou et al. 2014). For the purpose of this study, the dataset is downloaded from the official website at https://sharaku.eorc.jaxa.jp.

Some of the heavy rainfall cases for the study region are selected and shown in Table 1. The random heavy rainfall cases selected are subject to the availability of the DPR data when it passed the study region.

Table 1. Heavy rainfall cases in the study region

	2015	**2016**	**2017**	**2018**
Total orbits	18	79	87	16
Total pixels	26019	128105	163885	37114

3.5 GSMaP

The Global Satellite Mapping of Precipitation (GSMaP) is a project sponsored by Core Research for Evolutional Science and Technology (CREST) of the Japan Science and Technology Agency (JST). The project activities are promoted by JAXA Precipitation Measuring Mission (PMM) Science Team. GSMaP is one of the Global Precipitation Measurement (GPM) JAXA standard products where the rainfall product is released in a global domain of 60^0N to 60^0S about four hours after observation. A daily dataset of GSMaP that comes in a grid resolution of 0.1^0 x 0.1^0 at temporal resolution of 1 hour was used in this study. The dataset for the

purpose of this study is downloaded from the official website at
.

3.6 Ground Observation Data

Ground observation from the existing meteorological stations by MMD is used in the validation processes. The 24-hour operating stations are responsible for observing all meteorological parameters following the guideline of the World Meteorological Organization (WMO). Table 2 shows the number of operating stations subject to observation dates that are used in this study for the validation process.

Table 2. Number of operating stations by MMD

Observation dates	Number of operating stations
20 January 2017	203
13 July 2017	230
04 November 2017	236
19 December 2017	232

4.0 METHODOLOGY

Rainfall observation from space has become the major interest among scientists to understand the rainfall amount and distribution modulated by the atmospheric situations. Higher spatial and temporal resolution observations that are available from the satellite are value added in the latest monitoring method. Observing the rainfall from the satellite platform was found to be an effective method especially for both land and ocean. Several estimation techniques using Visible (VIS) and Infrared (IR) channels in geostationary satellite have long been introduced since 1970s. Recently, new development of a so-called hybrid or merging technique between Microwave (MW), IR and VIS imagery paves the efforts to improve the *instantaneous rainfall retrievals.* Integration methods between IR and MW have been developed to improve the algorithm to estimate the rainfall over land and

6

ocean such as established in Gairola and Krishnamurti (1992), Gairola et al. (2004), Mishra et al. (2010) and Kubota et al. (2007). New algorithms by merging in-situ observation with satellite retrieved precipitations have been developed in the works of Huffman et al. (2007), Adler et al. (2003) and Gairola et al. (2015). INSAT Multispectral Rainfall Algorithm (IMSRA) is one of its kind using integration methods that have been developed by Indian Space Research Organization (ISRO). The algorithm was developed as a specific technique to estimate the rainfall for the Tropical Indian Ocean region at both land and ocean using the regression between the mean Precipitation Radar (PR) and the Brightness Temperature (BT) from TIR, Gairola et al. (2010).

4.1 IMSRA rainfall algorithm

The precipitation rate of BT-TIR was derived from the best fit law between instantaneous TRMM precipitation radar (TRMM-PR) surface rain estimates and satellite BT-TIR at cloud top. The satellite Kalpana BT-TIR from the cloud top was collocated with the PR-derived rainfall rate in a 0.25^0 x 0.25^0 grid over the Indian region within the observation domain in between the latitude and longitude of 20^0S to 40^0N and 50^0E to 120^0E, respectively. The regression between the mean PR derived rainfall rate and BT-TIR was calculated and the equation representing the regression was used from Gairola et al. (2010). The algorithm was specifically designed to estimate rainfall over the Indian summer monsoon region. IMC rain product is an improved version of IMSRA studied by Mahesh et al. (2014) that incorporated a three tier correction scheme to the parent IMSRA algorithm. The correction schemes applied in the new version are (i) global calibration bias correction that was designed on the basis of comparison with TRMM-3B42 daily average rain, (ii) climatological ratio bias between IMSRA and TRMM- 3B42 for the orographic regions and (iii) the global bias correction. Cloud growth correction is computed based on the evolution of clouds computed from two consecutive IR images. The average bias between the rain estimates of TRMM-3B42 and IMSRA rain is absorbed into a polynomial model. Orographic correction is computed on the basis by Mahesh et al. (2014). Furthermore, a cloud cooling index correction

7

is incorporated in the algorithm based on studies by Mahesh et al. (2014). This three-tier correction scheme is incorporated into an operational IMSRA algorithm (Gairola et al. 2016).

IMSRA has been successfully experimented using BT-TIR at wavelength 10.5 μm to 12.5 μm from INSAT-3D to estimate the rainfall on summer monsoon (Prakash et al. 2010) and to estimate the rainfall during very severe cyclonic events (Bushair and Gairola, 2013). The algorithm has been experimented beyond the tropical Indian region and the acceptable result was observed. The rainfall estimation by IMSRA was found acceptable when it was applied over Malaysia region during severe rainfall episodes. Figure 1 shows that the estimates by IMSRA have produced a good rainfall distribution map during severe rainfall on 23 December 2014 (Shaari and Gairola, 2018). The correlation coefficient between the estimates by IMSRA and TRMM/GSMaP was more than 0.8 at all extreme cases. The rainfall signature over South China Seas (SCS) was clearly visualized by the model and it is believed to be the precursor of the severe rainfall episodes on next following day on 24 December 2015. These continuous rainfall events had caused severe floods on 25 December 2015 that had almost 90,250 people evacuated. These good results triggered the urgency to conduct further studies about utilizing the algorithm using different input parameters from satellite Himawari that is continuously monitoring the Malaysia region.
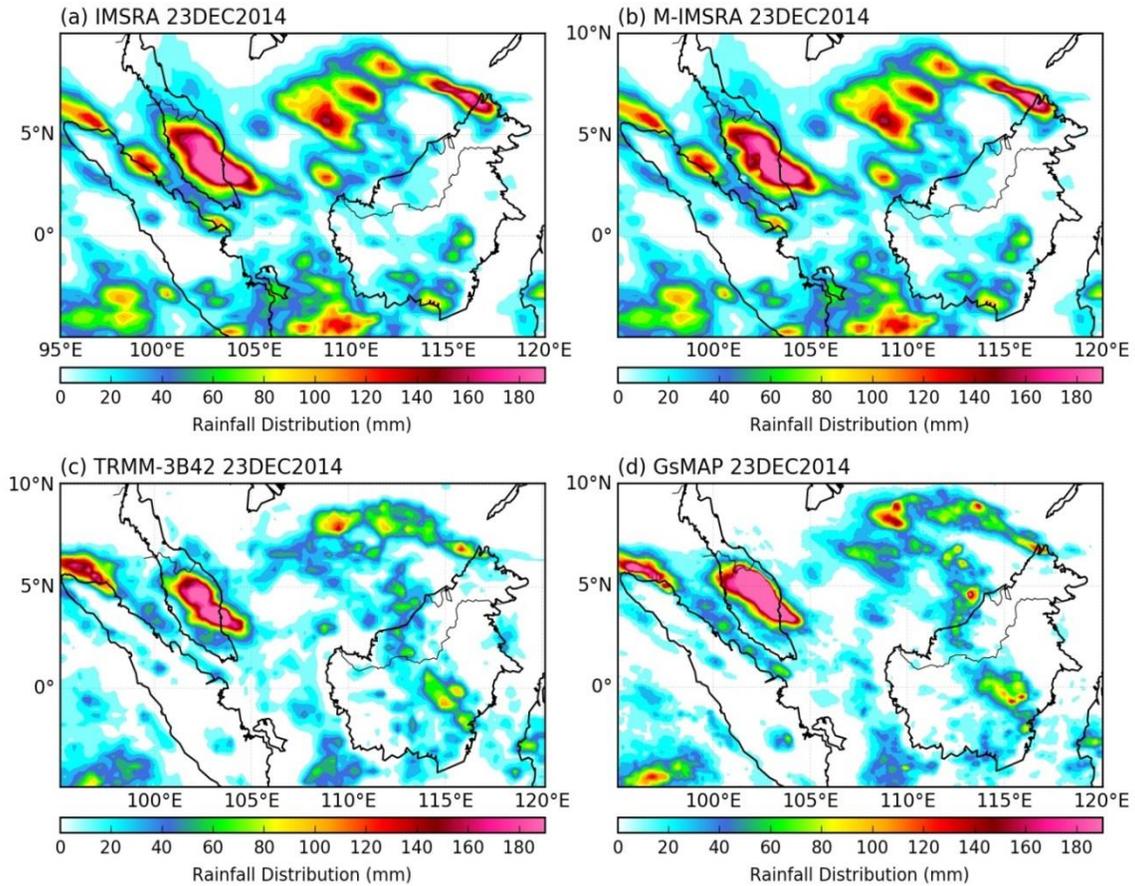
Figure 1.Rainfall map on 23rd December 2014

4.2 Rainfall map distribution

In order to evaluate the algorithm and rainfall distribution over Malaysia region, a sample of heavy rainfall events is chosen. Four observation dates which is on 20 January 2017, 13 July 2017, 04 November 2017 and 19 December 2017 that observed higher rainfall amount of more than 40 mm, were analyzed. Rainfall estimation using regular IMSRA and the corrected version of Global Bias Correction (IMR1), Cloud Growth Correction (IMR2) and the combination of Global Bias Correction with Cloud Growth Correction (IMR1-IMR2) were performed to observe the rainfall distribution qualitatively and quantitatively. The method that provides better results is chosen for further discussion. Rainfall map of daily, exact hourly and average hourly was plotted and discussed in detail. The idea behind plotting the hourly rainfall map is to evaluate how these models could benefit the

9

now-casting applications in the region. Table 3 shows the hourly rainfall of more than 40mm recorded on the respective dates at each meteorological station.

Table 3. Hourly rainfall observed at MMD stations

Stations	Latitude	Longitude	Events	Hour (UTC)	Amount (mm)
48601	5.2969	100.2722	04 Nov. 2017	1100	47
48602	5.4572	100.3883	04 Nov. 2017	0800	50.4
41529	5.35	100.4	04 Nov. 2017	1200	63.8
41543	5.65	100.5	04 Nov. 2017	0900	52.3
40587	5.8167	102.05	04 Nov. 2017	0800	43.8
49476	4.7519	103.4147	04 Nov. 2017	1100	43.8
97426	4.4167	118.0167	19 Dec. 2017	1600	56.9
96481	4.3161	118.1189	19 Dec. 2017	1600	50.8
43418	4.5833	101.0167	20 Jan 2017	1200	51.6
48625	4.5667	101.1	20 Jan 2017	1200	58.8
40586	5.7667	102.2	20 Jan 2017	0400	45.6
48617	5.7967	102.485	20 Jan 2017	1300	63.4
48649	3.05	103.0833	20 Jan 2017	0900	56
48657	3.7722	103.2119	20 Jan 2017	1100	40.6
96449	4.3333	113.9833	20 Jan 2017	1300	43.2
95612	4.8914	115.2044	20 Jan 2017	1000	43.6

5.0 RESULT AND DISCUSSION

5.1 Relationship BT-TIR of satellite Himawari and INSAT3D

Thermal infrared for both satellites Himawari (band 13) and INSAT3D (band 6) was randomly selected to observe their relationship. Table 4 shows the rainfall events and the average coefficient values that were applied for the correction of Himawari TIR with respect to INSAT3D. New corrected TIR of Himawari is calculated using the linear equation, $y = 0.9533(x) + 10.767$. Where x and y is the original and corrected BT, respectively. Total pixels of 120,000 points representing the entire observation domain were used and the results showed a good relationship between both datasets. The estimates using the corrected BT-TIR were compared and analyzed with the original BT-TIR by INSAT3D. The sample of the regression plot between BT-TIR of Himawari and INSAT3D is shown in Figure 2.

Table 4. Rainfall events for observing BT-TIR of Himawari and INSAT3D

No	Observation date	Time (UTC)	Regression		Correlation Coefficients
			Interception (K)	Slope (K)	
1	01May2016	0630	36.639	0.868	0.84
2	15Jul2016	0830	36.88	0.862	0.91
3	18Jul2016	0730	24.8	0.901	0.91
4	29Nov2016	0430	20.407	0.92	0.91
5	26Dec2016	0830	10.134	0.954	0.94
6	14Jan2017	1430	14.152	0.945	0.92
7	02Feb2017	0900	-12.973	1.034	0.93
8	27Jun2017	1430	38.046	0.859	0.90
9	14Nov2017	0930	-2.574	0.999	0.90
10	19Nov2017	2000	8.779	0.962	0.93
11	01Dec2017	1730	19.935	0.92	0.93
12	24Dec2017	1000	-12.292	1.035	0.93
13	11Jan2018	1700	-18.58	1.054	0.94
14	12Jan2018	0430	-12.613	1.035	0.95
Average			10.767	0.953	0.92

Brightness Temperature Between INSAT3D and Himawari-12JAN2018_0430

Total Pixel Counts = 120000
Correlation Coefficient =0.95
Interception =-12.61
Slope =[1.04]
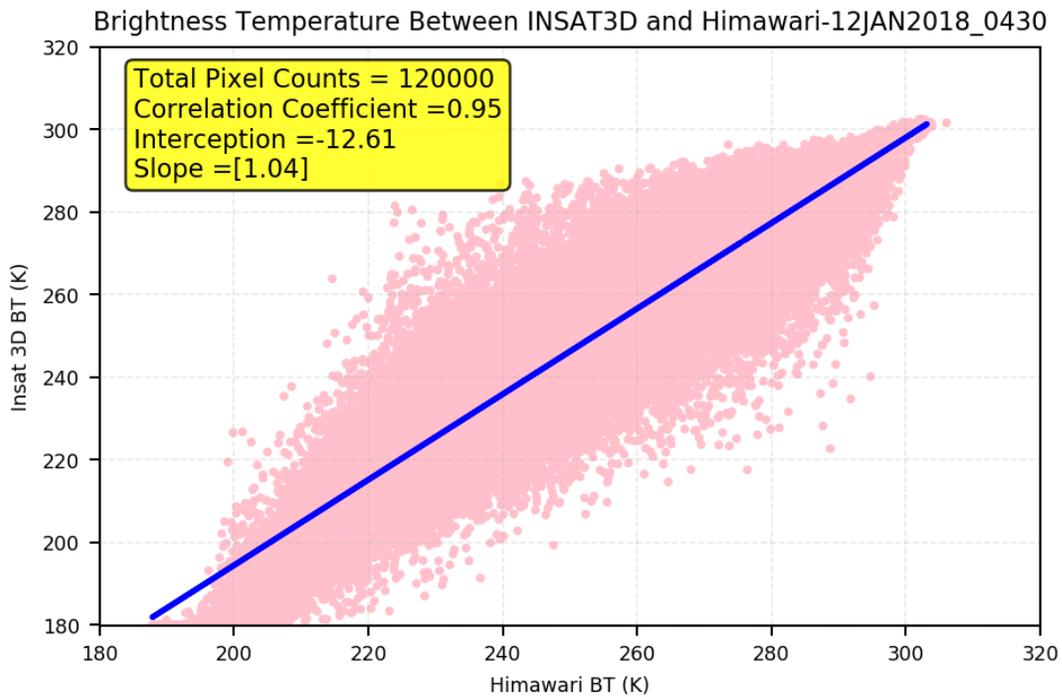
Figure 2. Regression plot between BT-TIR of Himawari and INSAT3D on 02 Feb 2017 at 0900UTC

5.2 Daily rainfall distribution by IMSRA and other correction models

Figure 3 shows the daily rainfall distribution on 20 January 2017 from the estimates by IMSRA and the corrected models of IMR1, IMR2 and the combination of IMR1-IMR2 using BT-TIR Himawari. The rain band clouds in northwest peninsular Malaysia and south Thailand were clearly visualized on all products except the intensity by IMR2 which was observed to be less than others. The rainfall intensity by IMR1 in northwest peninsular Malaysia, south Thailand and South China Seas was observed to be on the higher side than any other methods. Generally, IMR2 produced low rain rate at both inland and ocean when compared to other models. The combination models of IMR1-IMR2 produced similar rate and distribution as compared to the regular IMSRA.
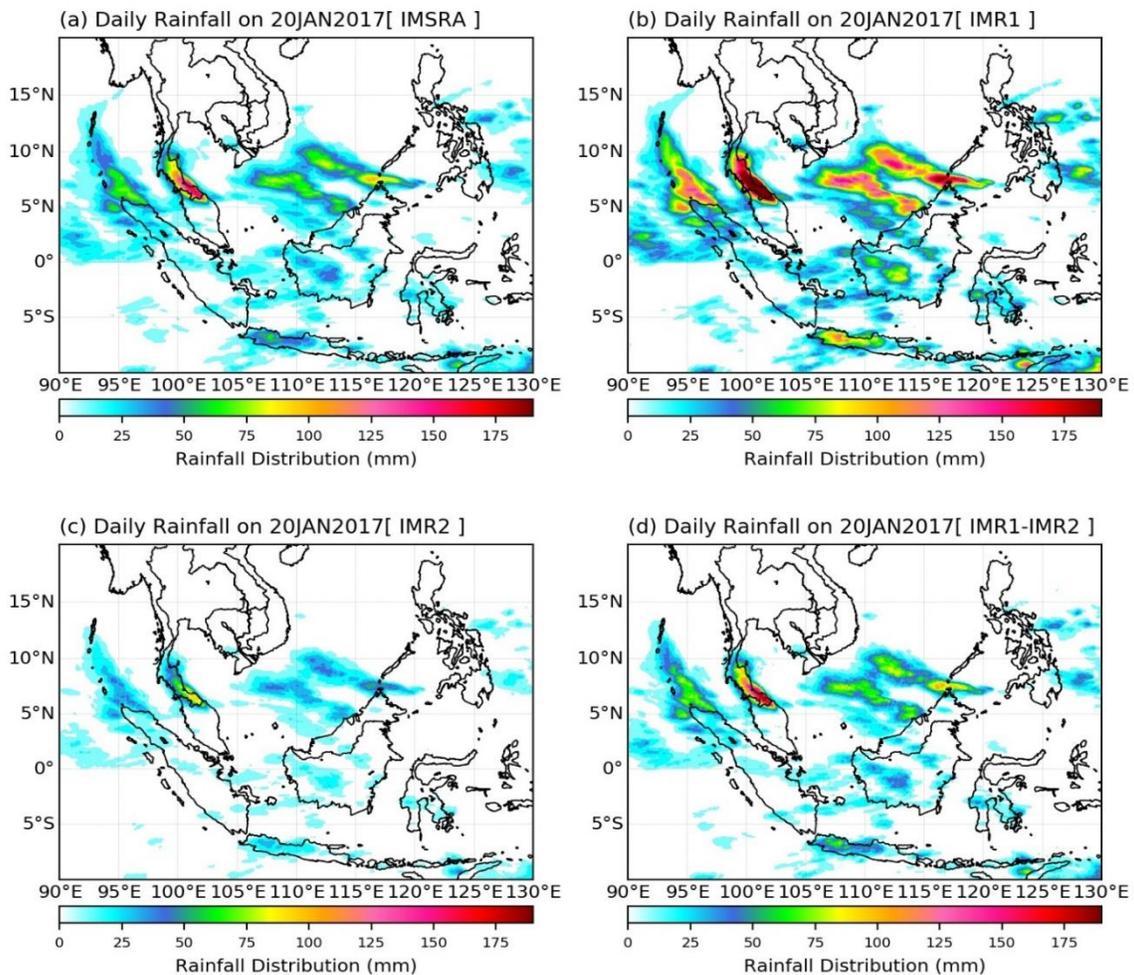
Figure 3. Daily rainfall distribution on 20 January 2017

Figure 4 shows the rainfall distribution map on 19 December 2017 for all the methods. Rainfall clouds were easily discriminated in all images. High rainfall rate of more than 175 mm was produced by IMR1 in South China Seas and Sabah coasts. The estimates by original IMSRA were observed to be closer to those given by the combination methods of IMR1-IMR2, whereas the same was found to be lower as compared to the rain rates from IMR2.
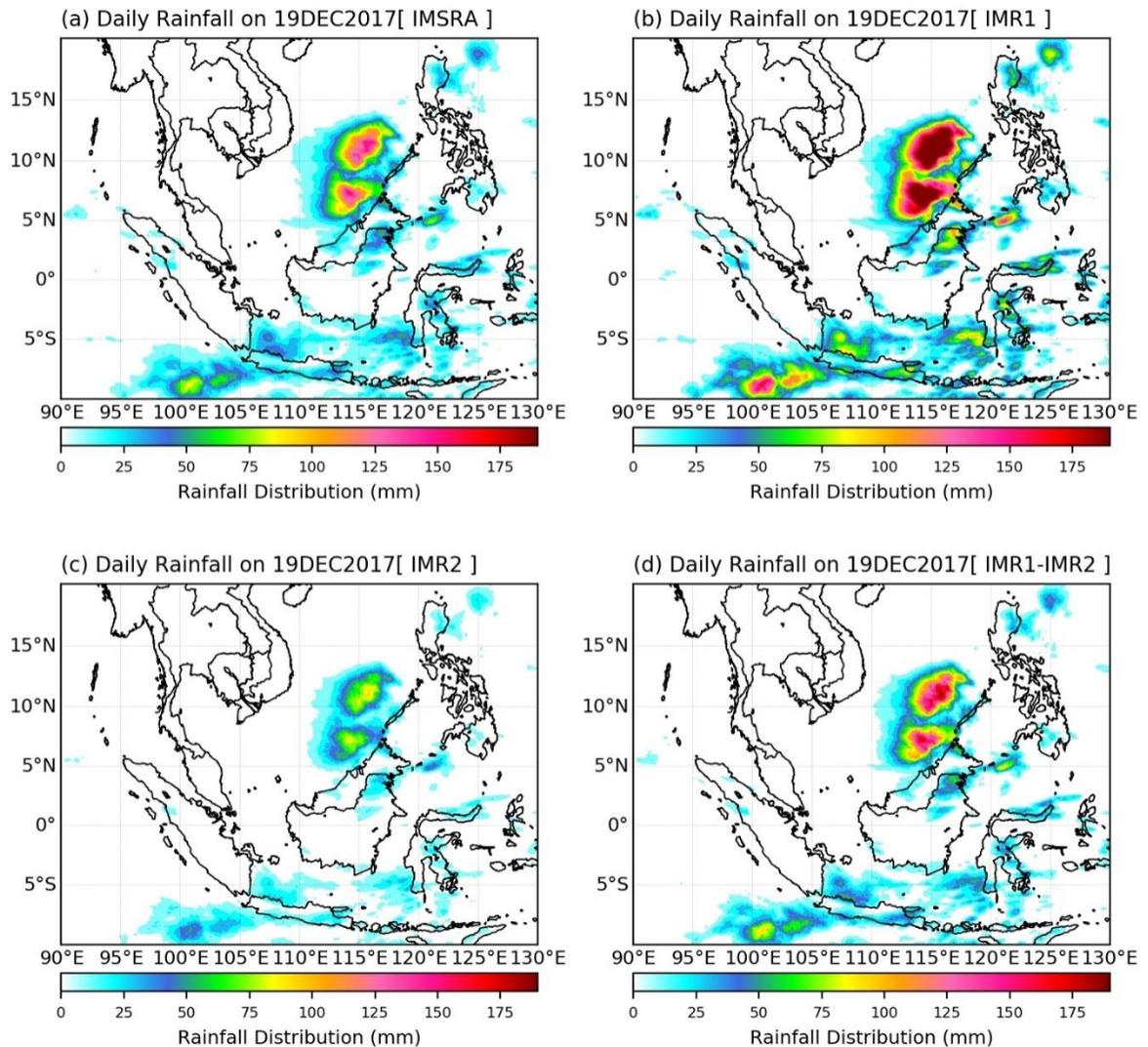
Figure 4. Daily rainfall distribution on 19 December 2017

13

5.3 Statistical comparison of daily rain rate between IMSRA and correction models with ground observation (without corrected BT-TIR)

The estimated rainfall on 04 November 2017 and 19 December 2017 in Figure 5 and Figure 6 respectively showed a higher correlation coefficient for regular IMSRA and IMR2 than any others. The correlation coefficient of the estimates by IMSRA showed higher values at 0.56 when compared to IMR2 at 0.55 for 19 December 2017. Correlations for both IMSRA and IMR2 were observed to be slightly lower for 04 November 2017. The correlations of the other two methods were relatively lower on both dates. Correlation coefficients for all methods on 13 July 2017 and 20 January 2017 were less than 0.4. Correlation coefficient on 13 July 2017 was the lowest for all estimation methods. Although the rainfall spikes were clearly visualized on the image, a thorough investigation should be conducted to identify the cause of the poor correlation. The estimated rainfall from some stations on 20 January 2017 was observed to be shifted as compared to the ground observation.
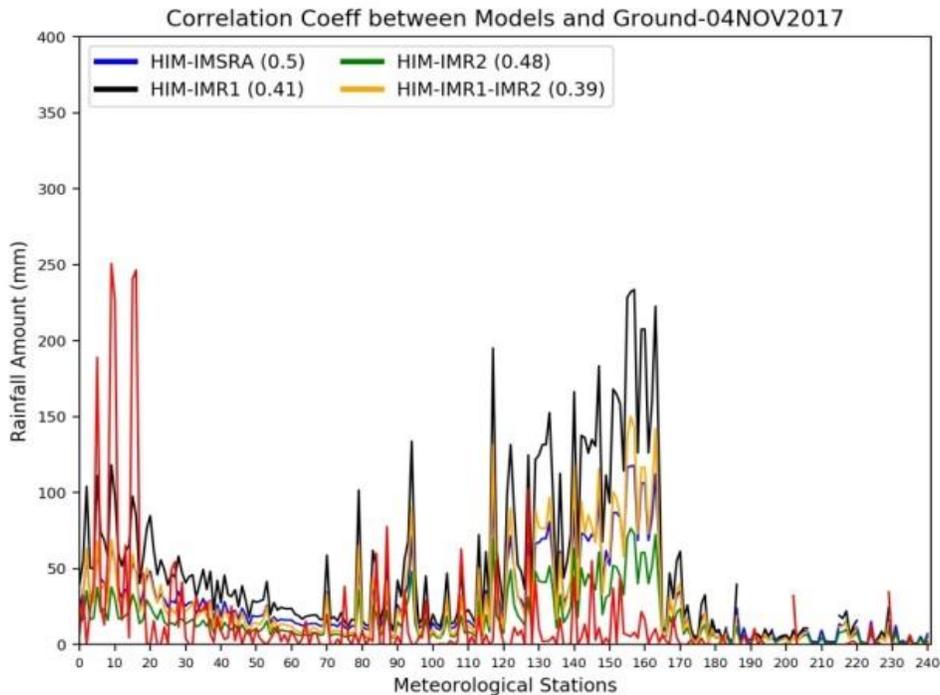
Figure 5. Correlation coefficient between models and ground on 04 November 2017. (Ground observation in red line)

14
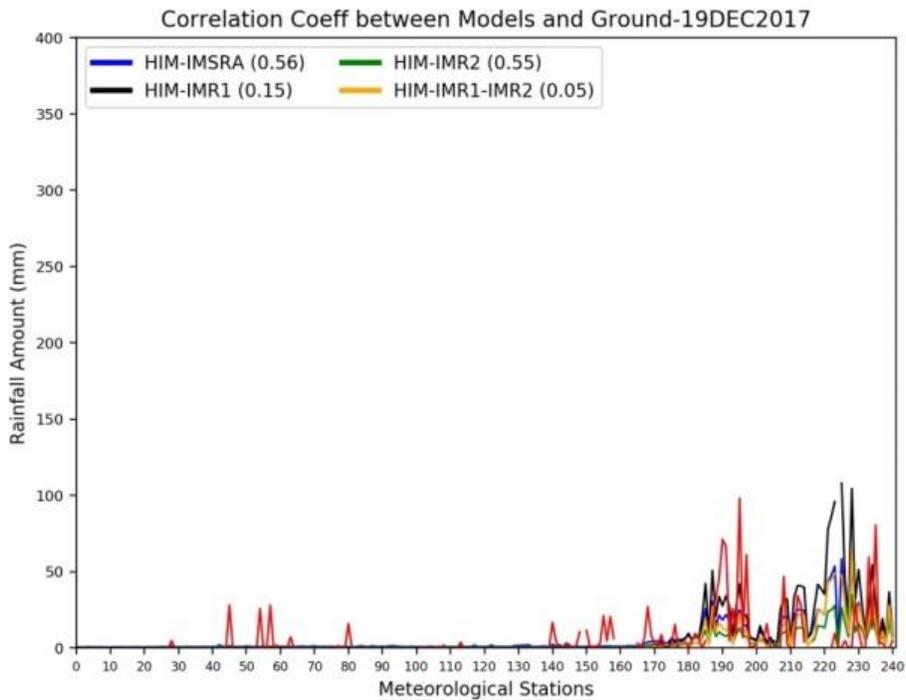
Figure 6. Correlation coefficient between models and ground on 19 December 2017. (Ground observation in red line)

5.4 Statistical comparison of daily rain rate between IMSRA and correction models with ground observation (with corrected BT-TIR)

Estimated rainfall using regular IMSRA was consistently showing higher correlation coefficient among other methods even after BT-TIR corrections. Higher correlation value of more than 0.5 was observed on 04 November 2017 (Figure 7) and 19 December 2017 (Figure 8). An estimated rainfall by IMR2 also showed a good correlation for the same dates but slightly lower than that regular IMSRA. The results for both regular IMSRA and IMR2 were slightly improved after correcting the BT; however the correlation coefficients on 13 July 2017 and 20 January 2017 were poor and insignificant.
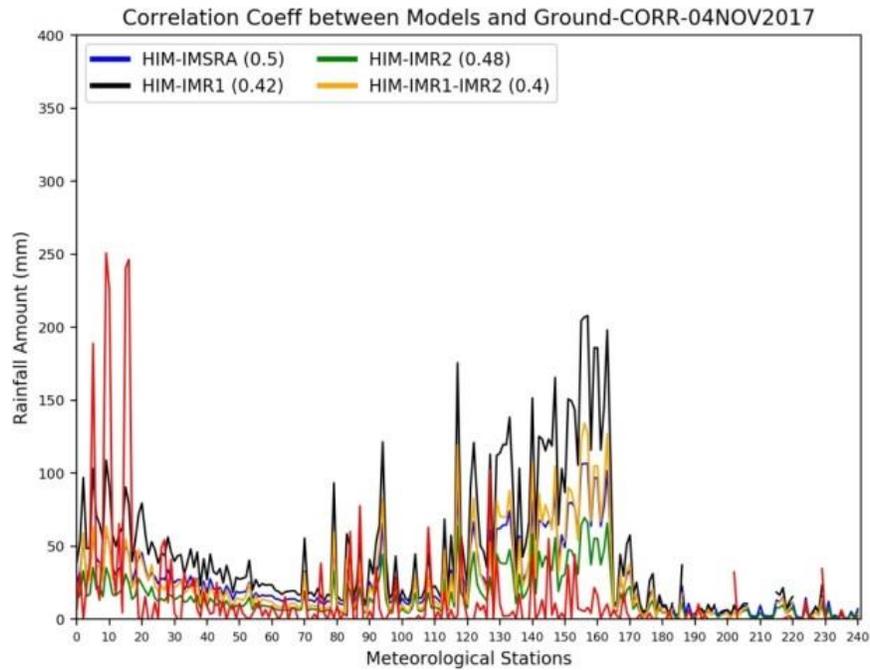
Figure 7. Correlation coefficient between models and ground on 04 November 2017 after corrected TIR. (Ground observation in red line)
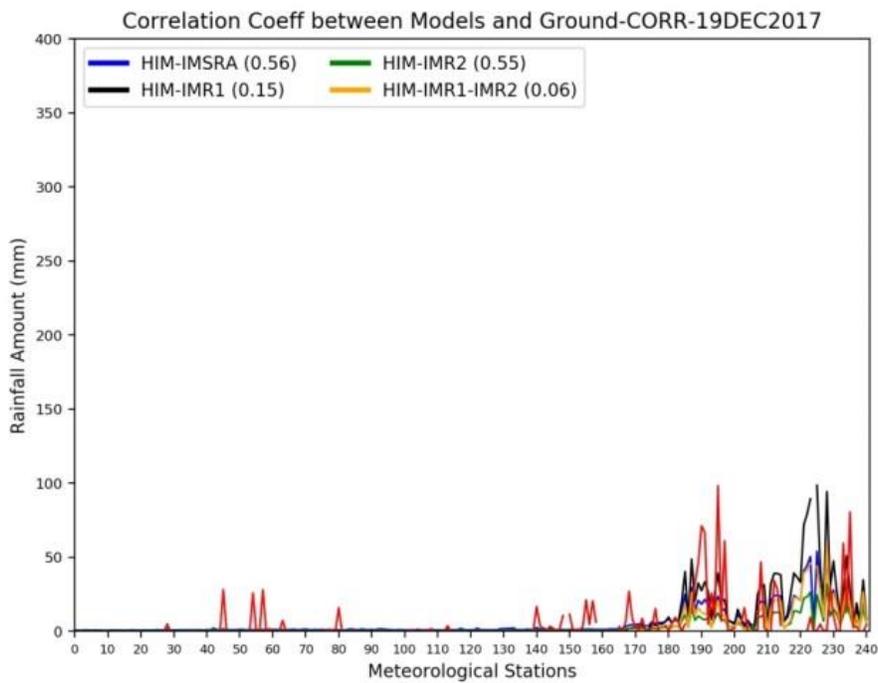
Figure 8. Correlation coefficient between models and ground on 19 December 2017 after corrected TIR. (Ground observation in red line)

16

5.5 Statistical comparison of daily rain rate from IMSRA and IMR2 with other satellite-derived products

5.5.1 Regular IMSRA

The rainfall estimation from Himawari showed a very good correlation of more than 0.5 on both dates on 04 November 2017 (Figure 9) and 19 December 2017 (Figure 10). The correlation coefficient of other derived rainfall products with the ground observations was found to be similar to those given by Himawari for both dates.

The correlation coefficient by INSAT3D was best at 0.57 on 19 December 2017 but slightly higher than Himawari at 0.56. Correlation coefficient on 04 November 2017 of Himawari was 0.5 slightly higher than that of INSAT3D at 0.48. Rainfall estimation by GSMaP was observed to be similar to that of Himawari at 0.5 on 04 November 2017; however, it recorded the lowest correlation (0.45) than the others for 19 December 2017. Correlation by GPM-IMERG was found lower than Himawari and INSAT3D on both dates of 04 November 2017 and 19 December 2017 but slightly higher than in GSMaP for 19 December 2017.The correlation of other methods for 13 July 2017 and 20 January 2017 was observed to be the lowest except for GSMaP that resulted more than 0.3.
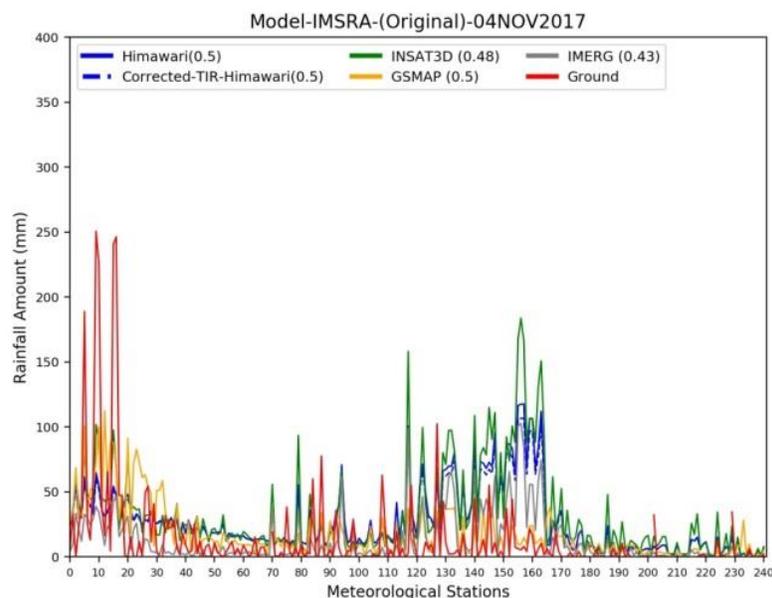

Figure 9. Correlation coefficient between IMSRA and other satellite-derived products on 04 November 2017.

17
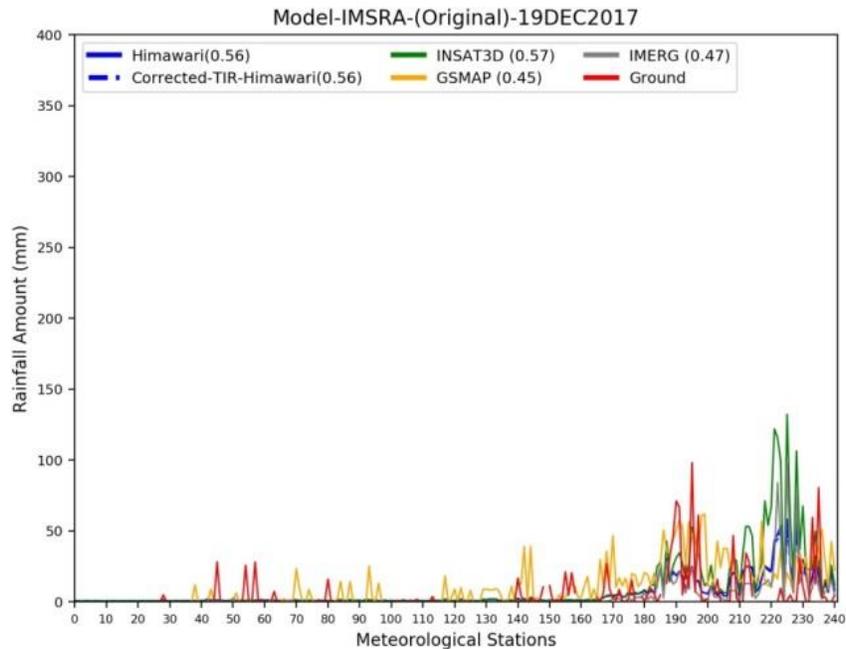
Figure 10. Correlation coefficient between IMSRA and other satellite-derived products on 19 December 2017

5.5.2 IMR2

The corrected TIR from Himawari did not show any significant results after being applied to this technique. The correlation coefficient between the actual and corrected BT-TIR on both 04 November 2017 (Figure 11) and 19 December 2017 (Figure 12) was almost similar to each other at 0.48 and 0.55 respectively. The correlation coefficient of INSAT3D with ground observation showed good results on both 04 November 2017 and 19 December 2017. The correlation on 19 December 2017 was observed to be the highest among any others at 0.57 but almost similar to Himawari on 04 November 2017. Correlation coefficient for GSMaP was the highest among others at 0.5 for 04 November 2017 but was the lowest on 19 December 2017. The correlation coefficient for GPM-IMERG showed values less than 0.5 on both observations on 04 November 2017 and 19 December 2017. Correlation coefficient of GSMaP was 0.34 for 13 July 2017 and 0.43 for 20 January 2017. Both correlation coefficients were observed to be the highest among any others for the observation dates.

18
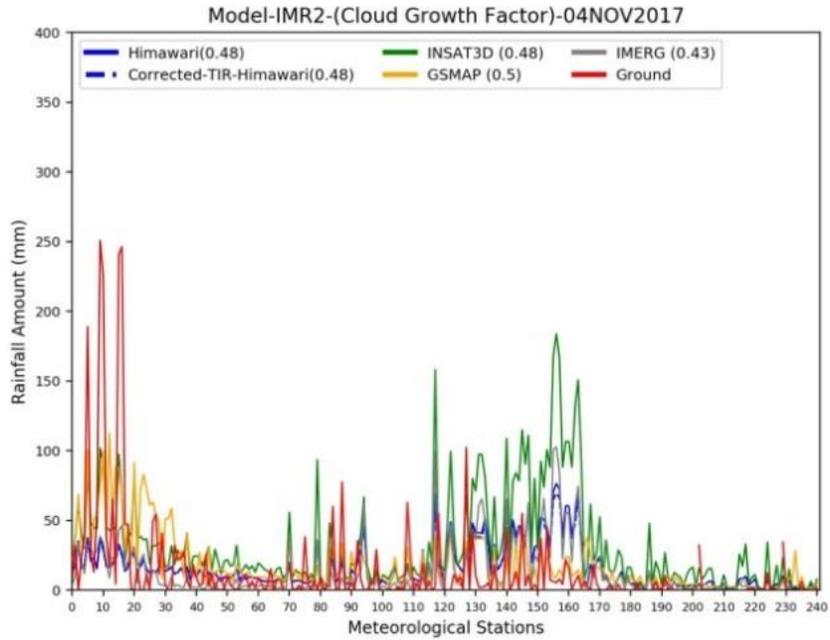
Figure 11. Correlation coefficient between IMR2 and other satellite-derived products on 04 November 2017
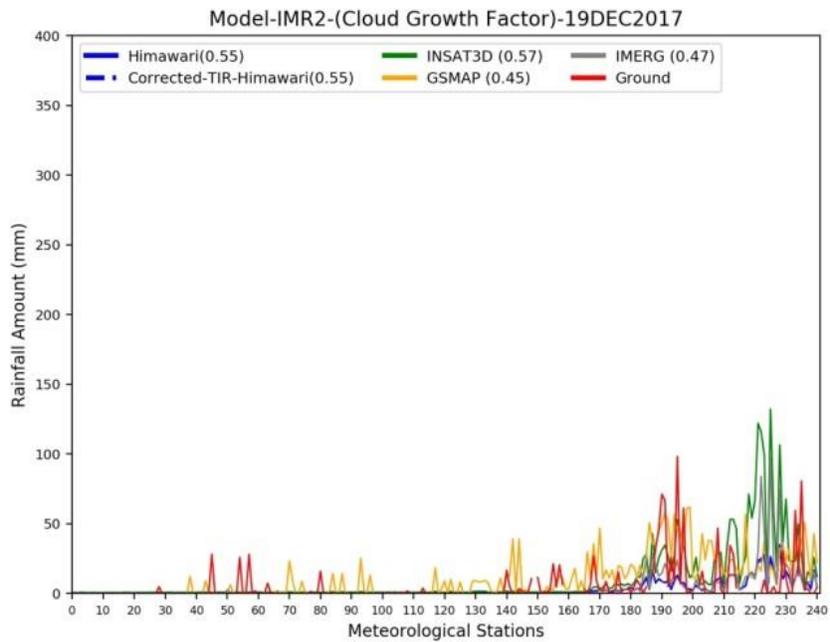
Figure 12. Correlation coefficient between IMR2 and other satellite-derived products on 19 December 2017

5.6 Statistical comparison between observation of exact and average hourly rain rates for IMSRA and IMR2 with satellite-derived products

5.6.1 Exact hour observation

The analysis from sections 5.4 and 5.5 suggested that only two estimation models of IMSRA and IMR2 have performed well on daily rainfall basis. From the previous sections, we observed that no significant changes were observed after applying the corrected Himawari BT-TIR. Hence, on that basis, only these two models with original Himawari BT-TIR are used for further discussion. The plot in Figure 13 shows the correlation coefficients of an exact hour rainfall estimation by both IMSRA and IMR2 between Himawari BT-TIR as input parameters and other satellite products from IMERG, GSMAP and INSAT3D.Total observation of 120,000 pixels has been collocated point to point between estimates and satellite-derived products. Correlation coefficient between INSAT-IMSRA was observed to be good compared to others at about 0.9. The correlation however was less in INSAT-IMR2 at about 0.6. The correlation coefficient between IMERG-IMSRA showed slightly lower values than that of INSAT-IMSRA at about 0.6. The relationship of INSAT-IMR2 also seemed better after being compared to IMERG-IMSRA. The result suggested that the estimates from BT-TIR in Himawari were able to produce good results as in the original BT-TIR in INSAT3D.
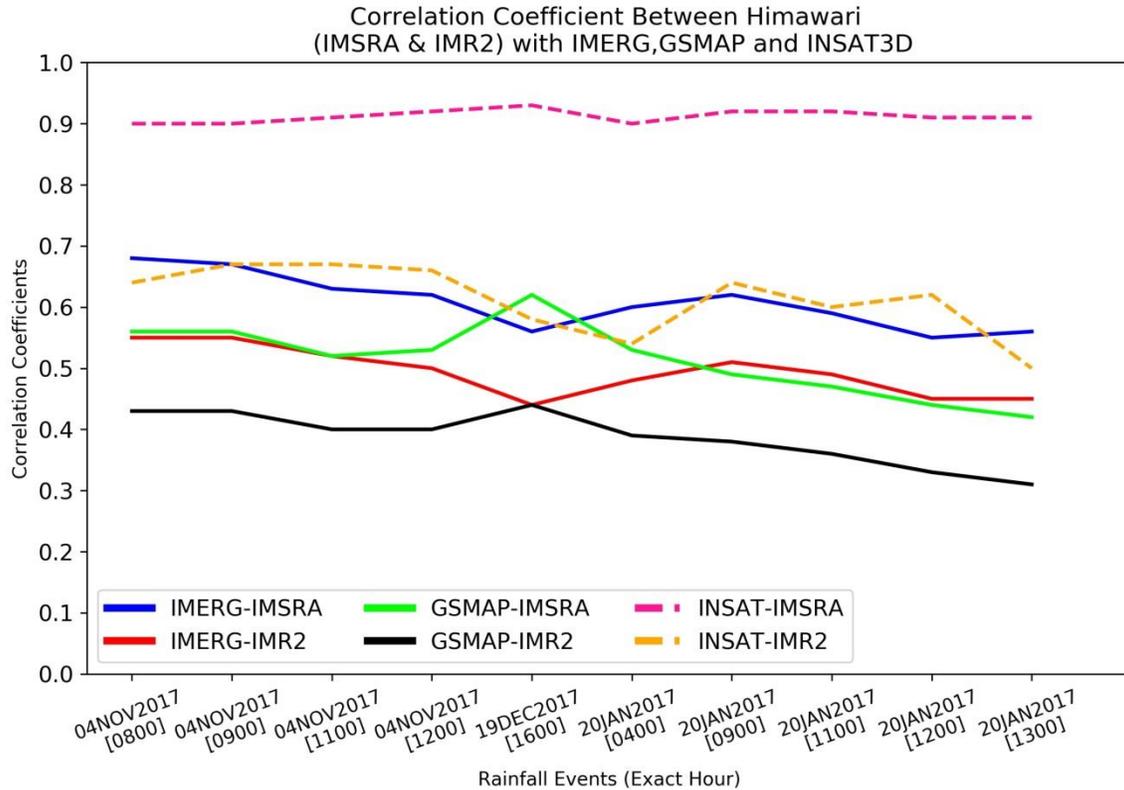
Figure 13. Correlation coefficient of IMSRA and IMR2 with other satellite-derived products for rainfall events (exact hour observation)

5.6.2 Average hour observation

Figure 14 shows the correlation coefficient distribution for IMSRA and IMR2 when compared with other satellite-derived rainfall products. Due to the difference in the temporal resolution offered by Himawari (10 minutes) and INSAT3D (30 minutes), the average hourly rainfall estimate was calculated. The estimates were spatially collocated with the hourly rainfall estimates provided by IMERG and GSMAP. The relationship between Himawari and INSAT3D in IMSRA was observed to be stronger with the correlation at 0.9 as compared to IMR2. Correlation coefficient for IMR2 was improved from about 0.6 to 0.8 as compared to the previous exact hour estimation in section 5.6.1. The relationship between Himawari and GSMaP was observed to be the lowest but consistent with both models, IMSRA and IMR2. Correlation coefficient between Himawari and IMERG was observed to have slightly changed after the estimates have taken the average values.

21
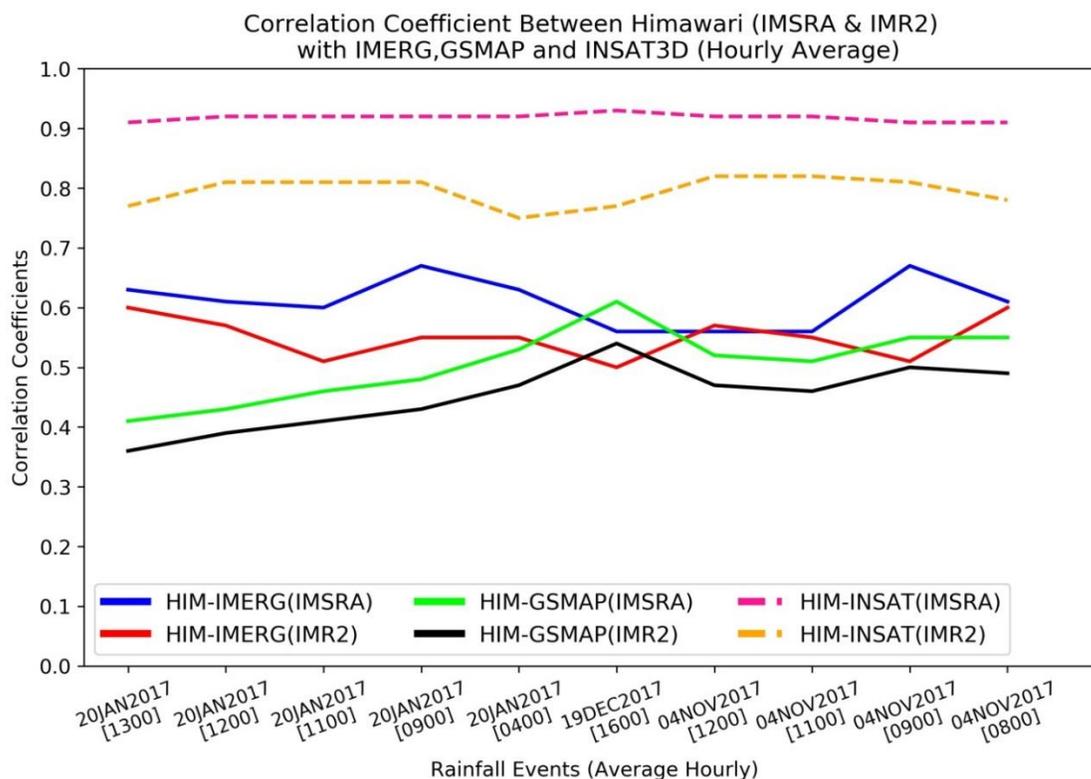
Figure 14. Correlation coefficient of IMSRA and IMR2 with other satellite-derived products for rainfall events (average hour observation)

5.7   Comparison of rainfall map and distribution of selected rainfall events for IMSRA with satellite-derived products

The plot in Figure 15 and Figure 16 shows the rainfall observed at exact and average hour, respectively. Sample rainfall estimates by IMSRA using Himawari BT-TIR at observation 1200 UTC on 04 November 2017 at spatial resolution 0.1 were plotted for discrimination. Figure 15 also shows that the MMD meteorological station at location code 41529 observed higher rain at 63.8 mm; however, our estimates were lower than this amount. The correlation between HIM-INSAT3D was observed as the highest at 0.92 than any other satellite-derived products. Figure 16 shows the hourly average estimates by IMSRA on the same observation date, which is on 04 November 2017. The rainfall intensity however did not change much when compared to the estimates at the exact hour. Higher rainfall cloud

pattern was observed to be similar in south peninsular Malaysia, west Kalimantan and north Philippines. All plots show rainfall cloud patches at station 41529 and rainfall amount between 15 and 20 mm.

Figure 17 shows that the rainfall observation on 19 December 2017 at 1600 UTC that was estimated by IMSRA using Himawari BT-TIR and INSAT3D dataset produced higher correlation coefficient at 0.93 than any other satellite-derived products. Station 97426 recorded higher rates at 56.9 mm but the estimates were slightly relocated from the point location. The relocation was clearly observed at both exact and average hour estimation as shown in Figure 17 and 18.
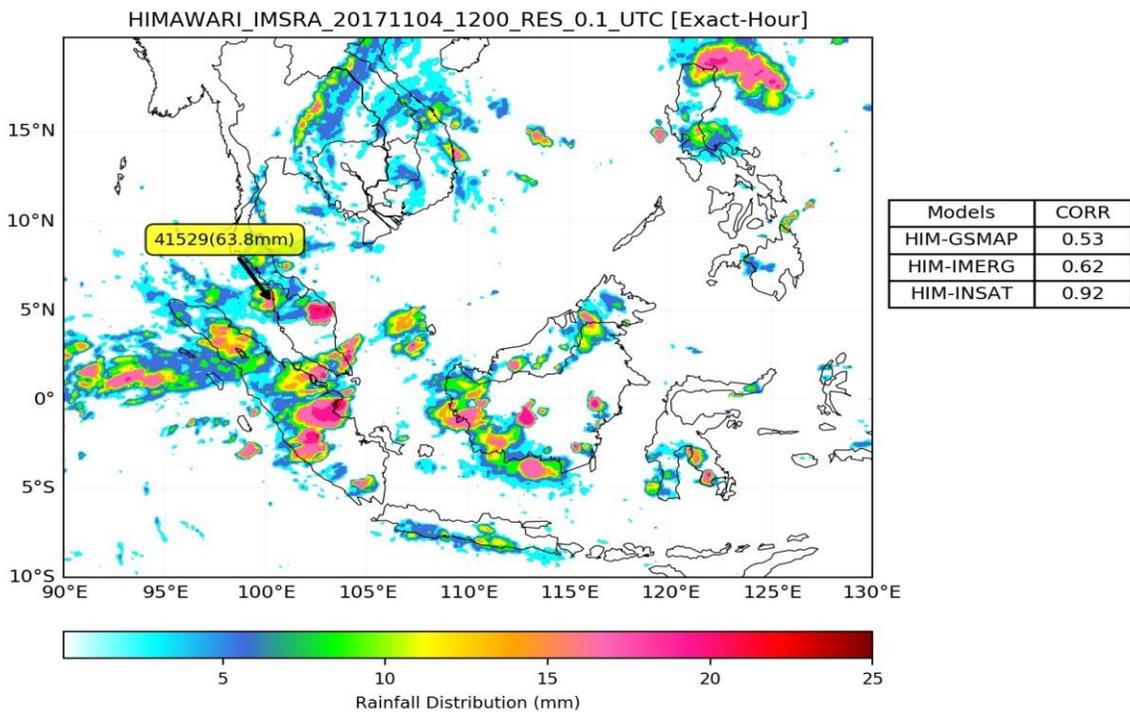
Figure 15. Rainfall distribution of exact time observation at 1200 UTC on 04 Nov 2017
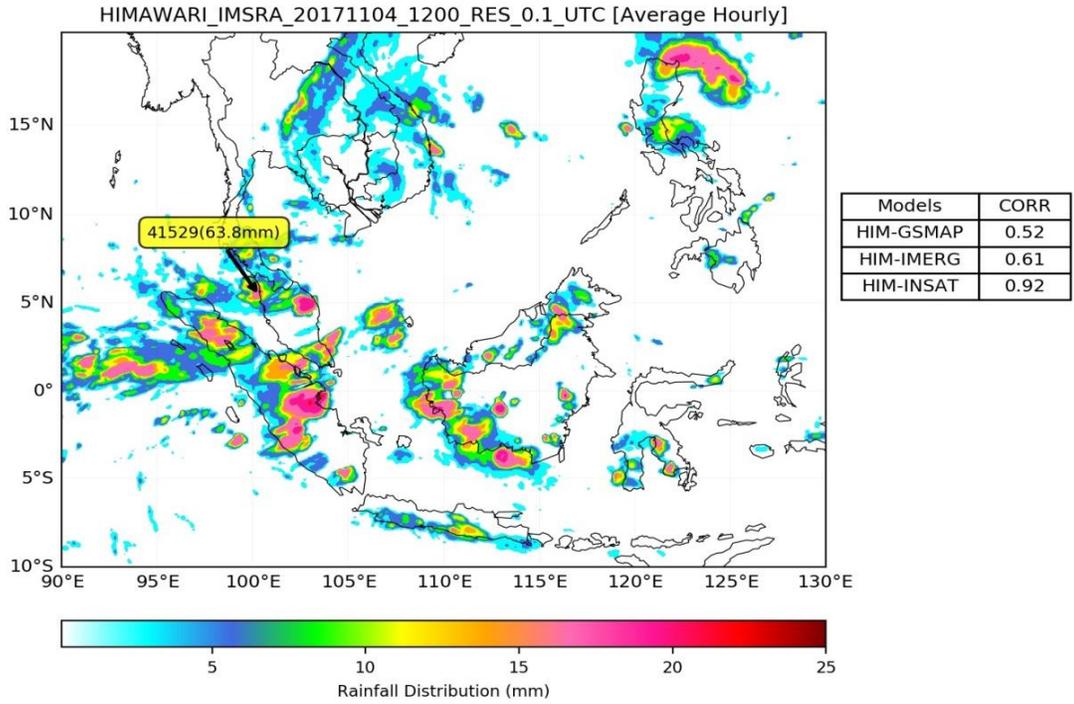
Figure 16. Rainfall distribution at hourly average observation at 1200 UTC on 04 Nov 2017
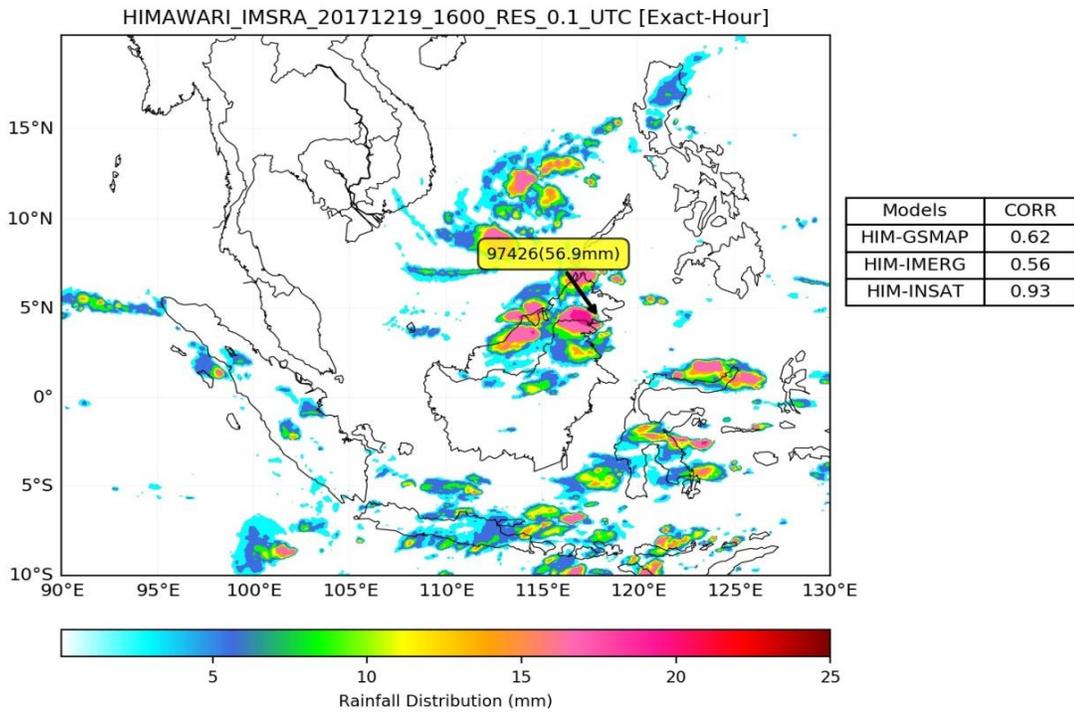
Figure 17. Rainfall distribution of exact time observation at 1600 UTC on 19 Dec 2017

24

HIMAWARI_IMSRA_20171219_1600_RES_0.1_UTC [Average Hourly]

Models	CORR
HIM-GSMAP	0.61
HIM-IMERG	0.56
HIM-INSAT	0.93

Rainfall Distribution (mm)
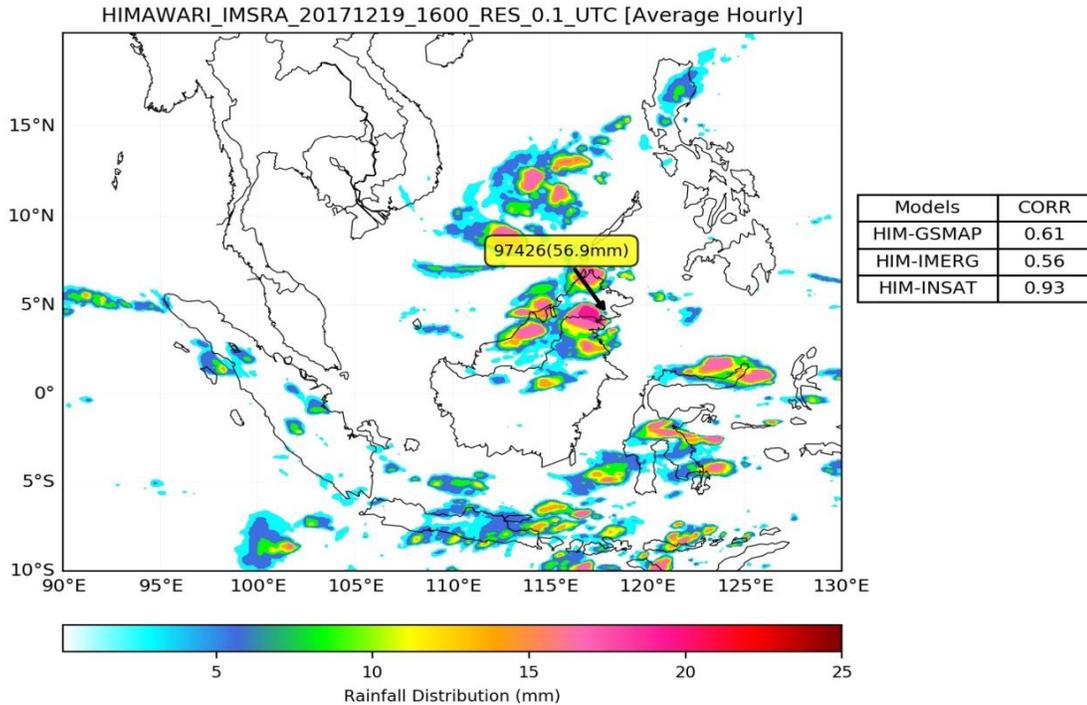
Figure 18. Rainfall distribution at hourly average observation at 1600 UTC on 19 Dec 2017

5.8 Comparison of rainfall map and distribution of selected rainfall events for IMSRA with actual satellite images.

Estimates by INSAT3D were observed to give higher rainfall rates than any other products. Rainfall cloud patches in Thailand, Laos and Sumatera were not captured in GSMAP but clearly visualized at MMD station in Figure 19. Generally, both GSMAP and IMERG produced similar rainfall distribution but some features were observed missing and some cloud patches were observed to be smaller when compared with Himawari and INSAT3D. The rainfall distribution by IMSRA for both Himawari and INSAT3D was found to bear the resemblance to the actual image of BT-TIR channel observed by Himawari satellite in Figure 20.
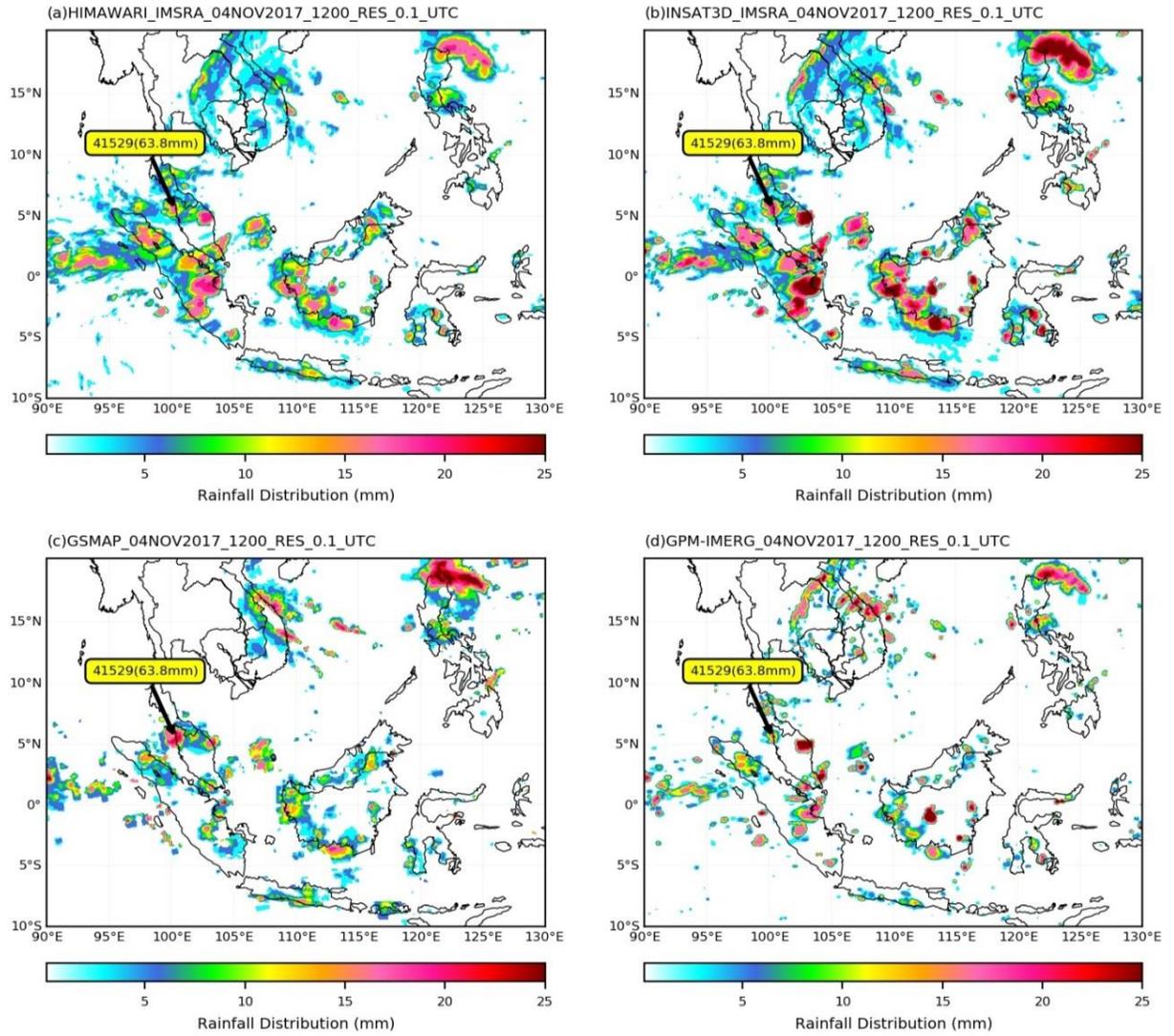
Figure 19. Comparison between Himawari and other satellite-derived products at 1200 UTC on 04 November 2017
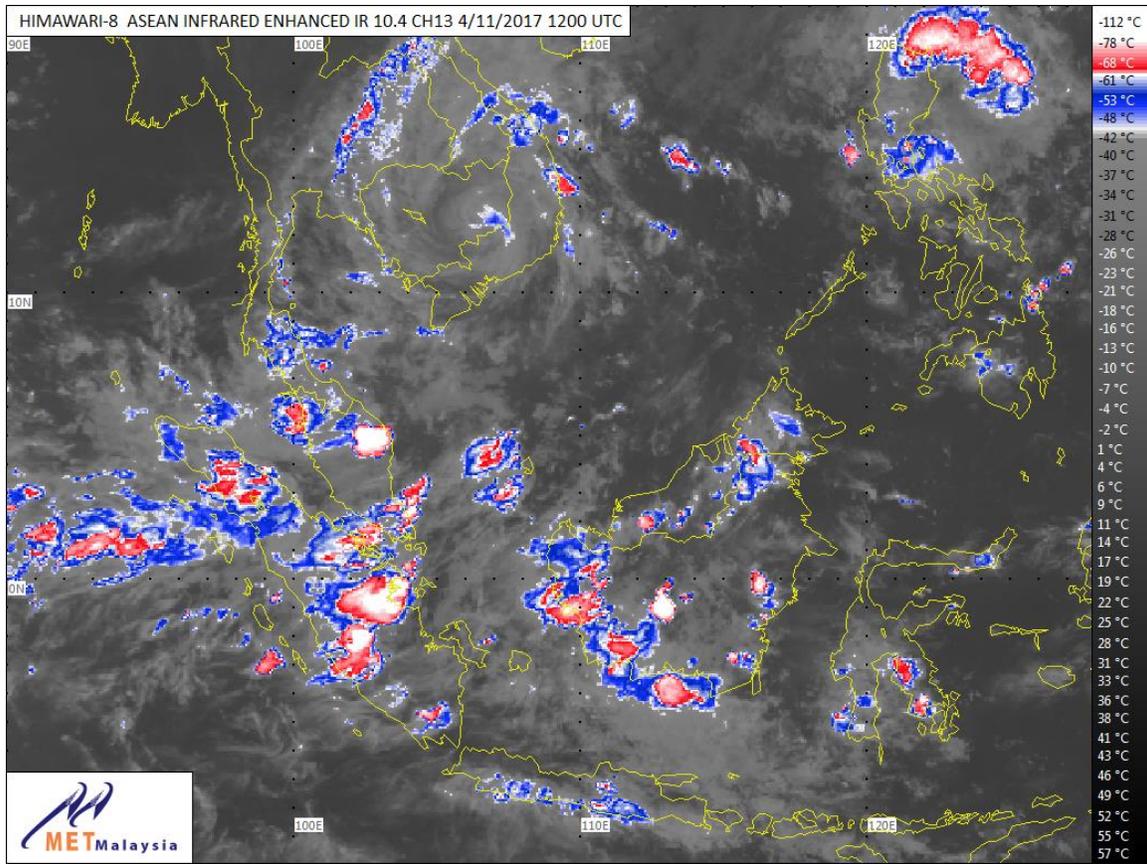
Figure 20. Actual satellite image on Himawari TIR channel at 1200 UTC on 04 November 2017

Figure 21 shows the comparison between the estimates and the actual image on 19 December 2017 at 1600 UTC. Similar cloud patches were visualized in both Himawari and INSAT3D datasets; however, the rain intensity as observed by INSAT3D was much higher than in Himawari. Rainfall clouds were less captured by IMERG particularly in Sarawak and Kalimantan. The features were also observed in South China Seas for all products. Rainfall distribution by IMSRA for both Himawari and INSAT3D was also found to resemble the actual image observed by the Himawari satellite in Figure 22.

27
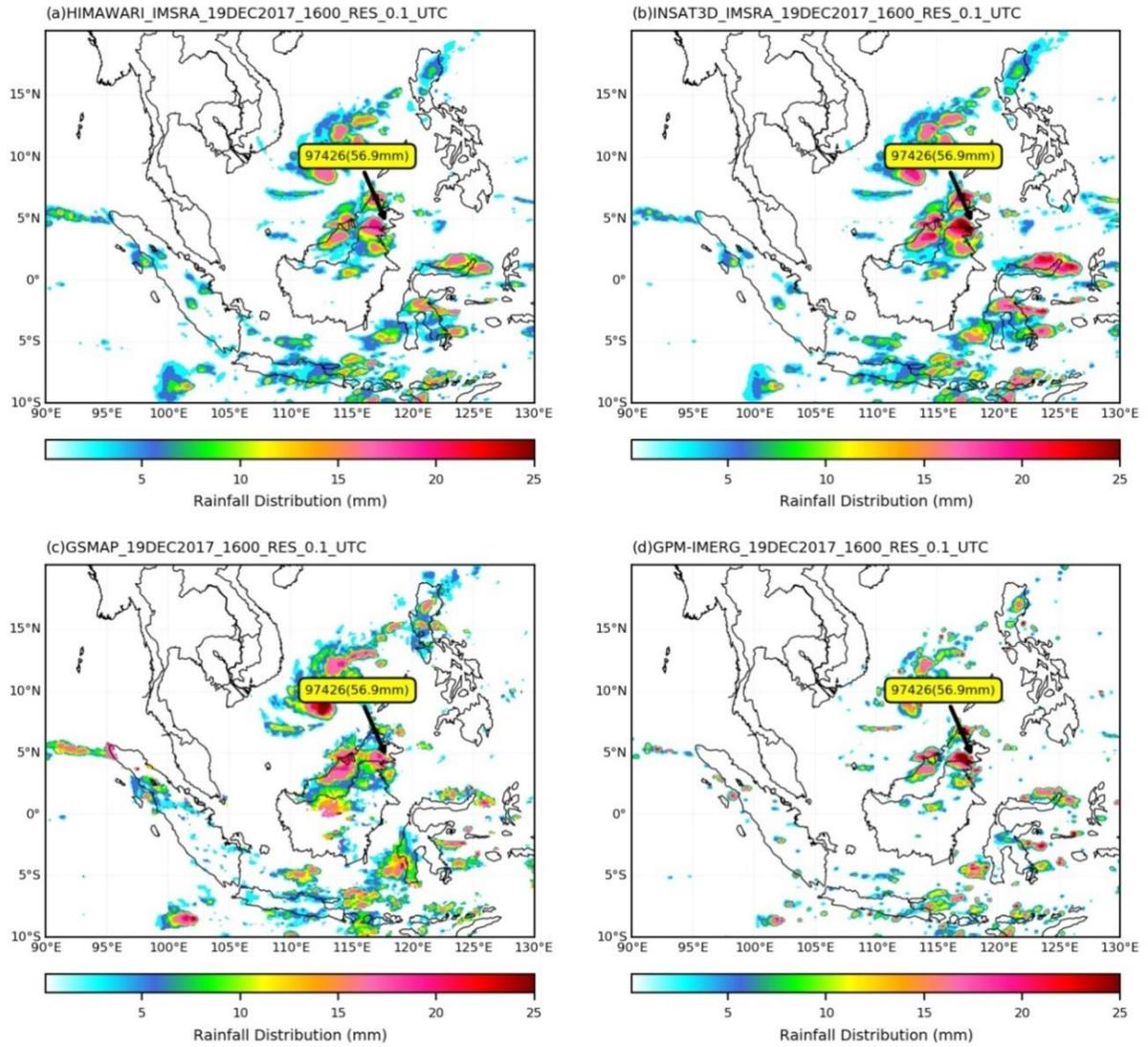
Figure 21. Comparison between Himawari and other satellite-derived products at
1600 UTC on 19 December 2017
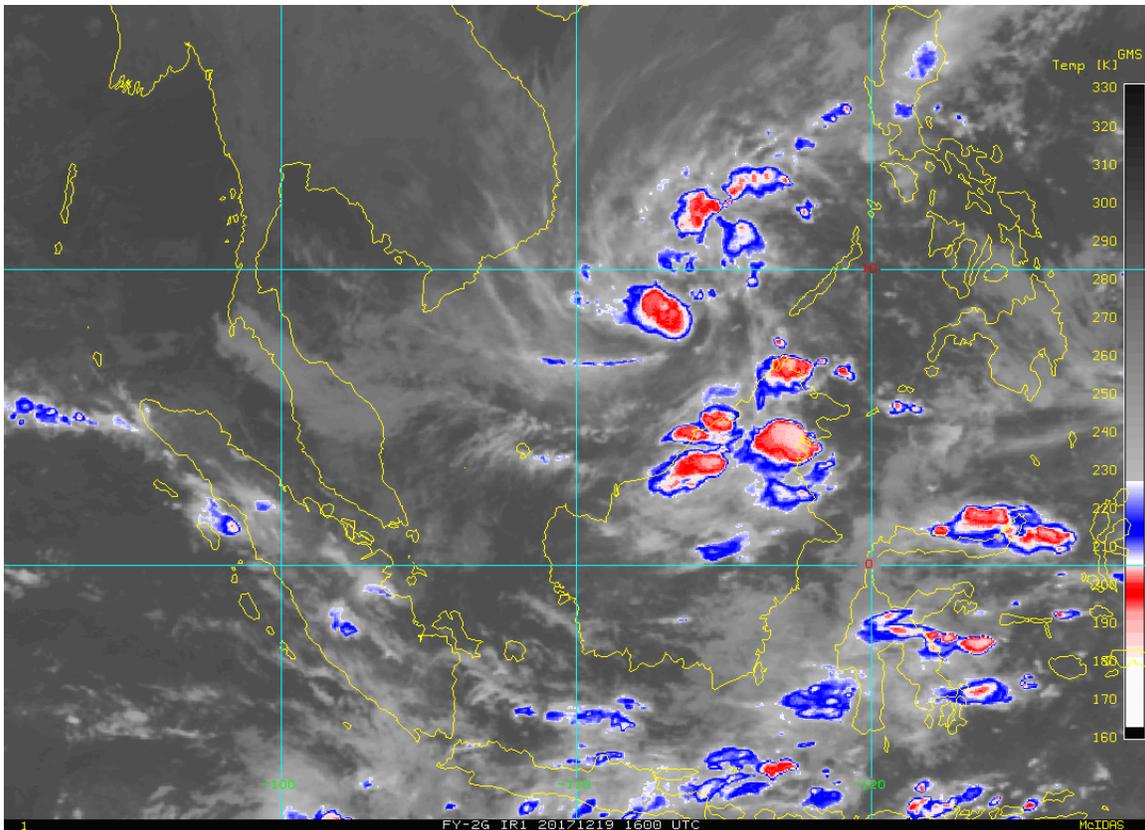
Figure 22. Actual satellite image on Himawari TIR channel at 1600 UTC on 16 December 2017

5.9 Comparison between ground observation with the estimates at both exact and average hourly observation

Figure 23 and 24 show the correlation coefficient between models and ground observation at both exact and average hour observation. Generally, the correlation coefficient for Ground-GSMAP was observed to be higher which is nearly at 0.5; however, the lowest reading recorded was on 20 January 2017 at 0400 UTC observation. Correlation coefficient for Ground-INSAT-IMSRA was found to be slightly higher than in Ground-HIM-IMSRA for both experiments.

29
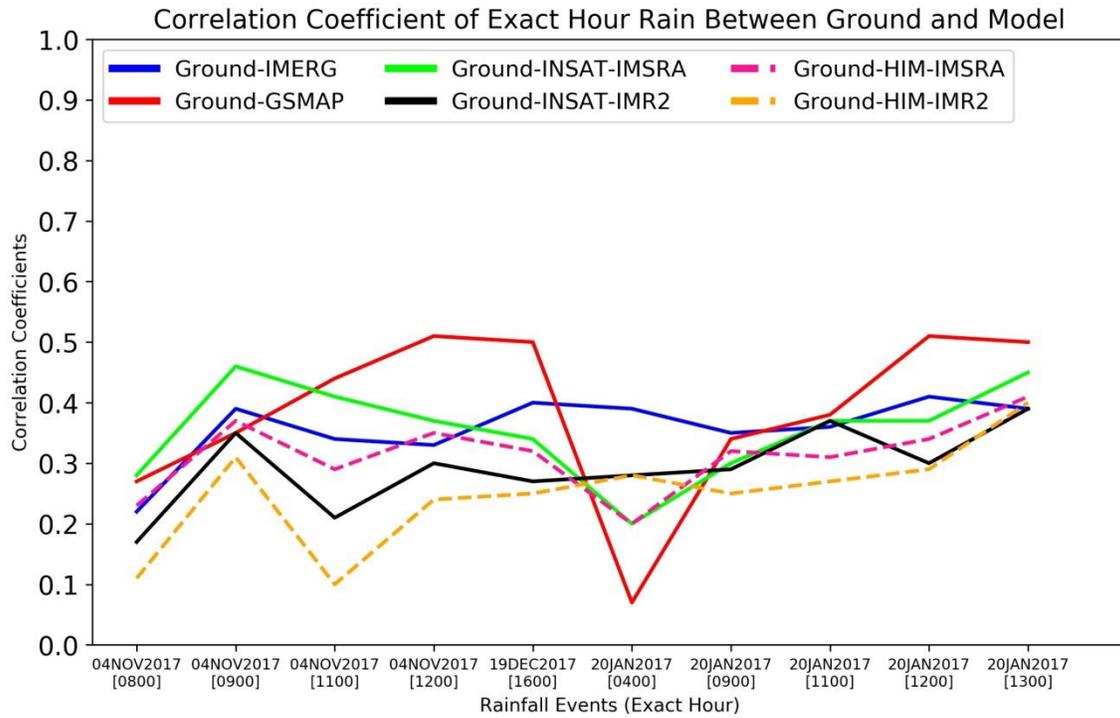
Figure 23. Correlation coefficient of exact hour between ground and models
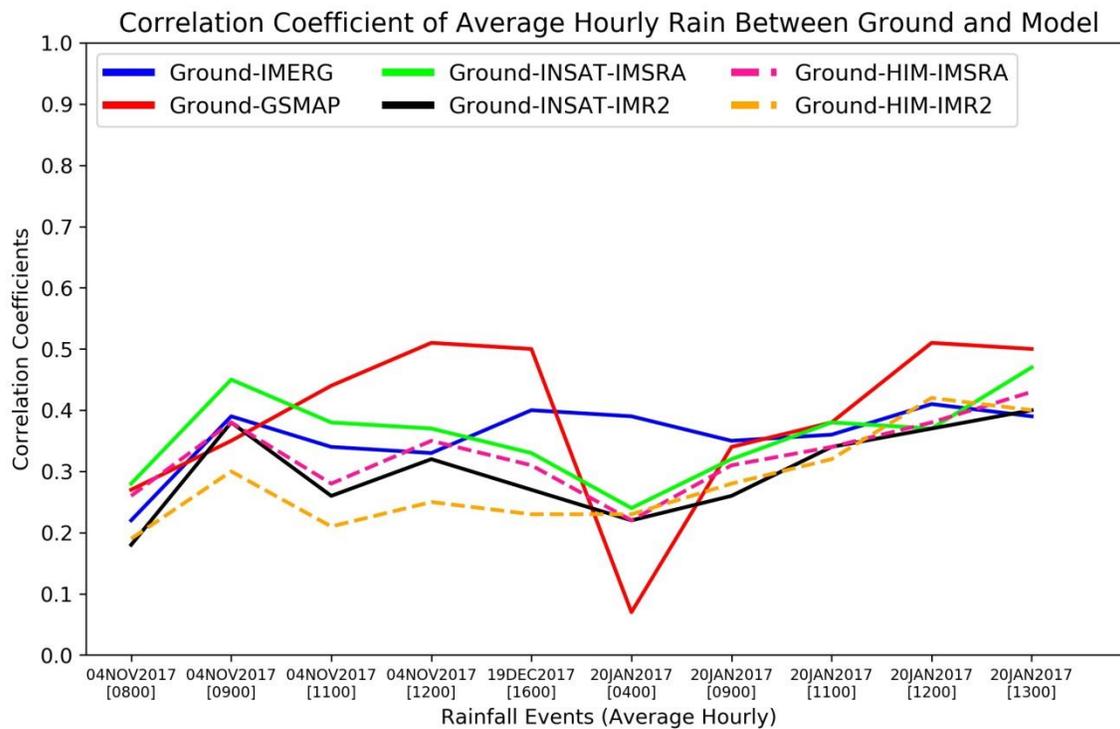
Figure 24. Correlation coefficient of average hour between ground and models

5.10   Rainfall distribution at each meteorological station

Figure 25 and Figure 26 show the rainfall distribution between the estimates and ground observation at the selected observation dates. It can be observed from both of the plots that the correlation coefficient between the ground and GSMAP was higher at 0.5 and more. The estimates by IMSRA for both Himawari and INSAT3D dataset have shown correlation coefficients in between 0.32 and 0.37, which is about similar to IMERG. The estimates by IMR2 were found weaker as compared to the other models at each day of observation.
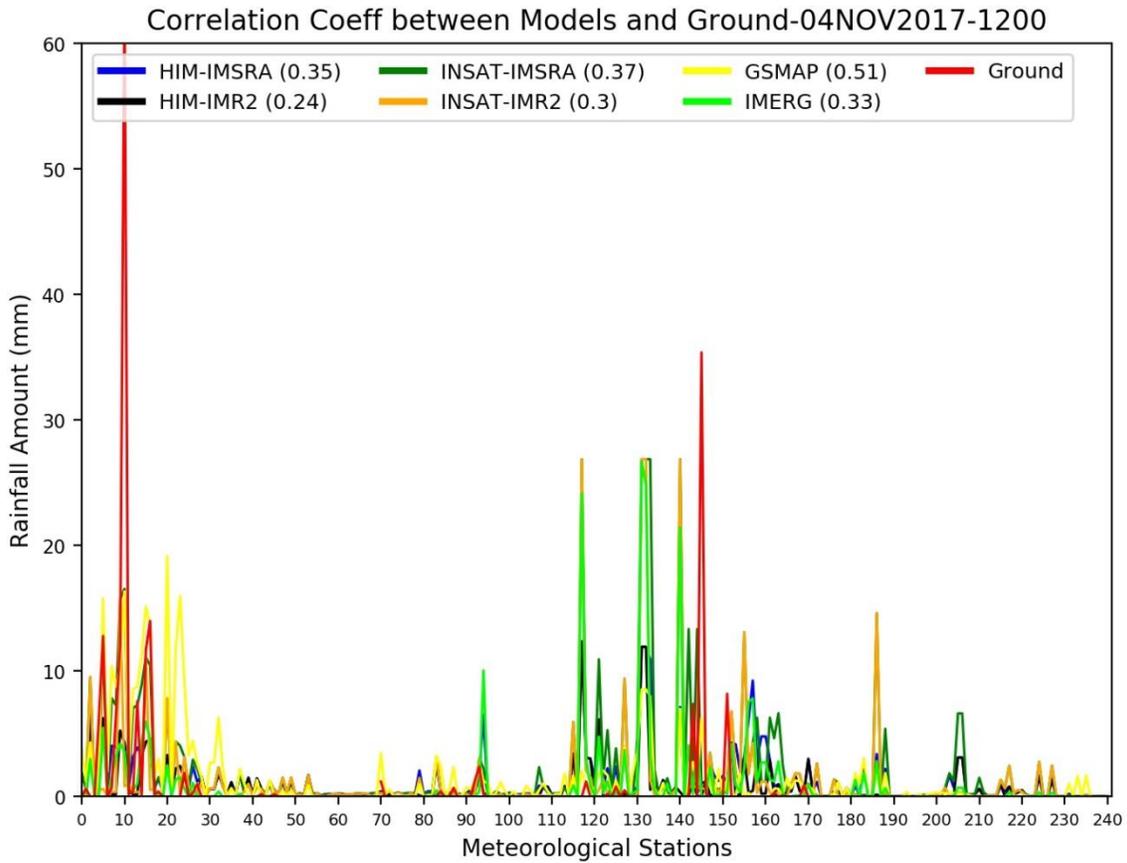

Figure 25. Rainfall distribution at meteorological stations on 04 November 2017 at 1200 UTC
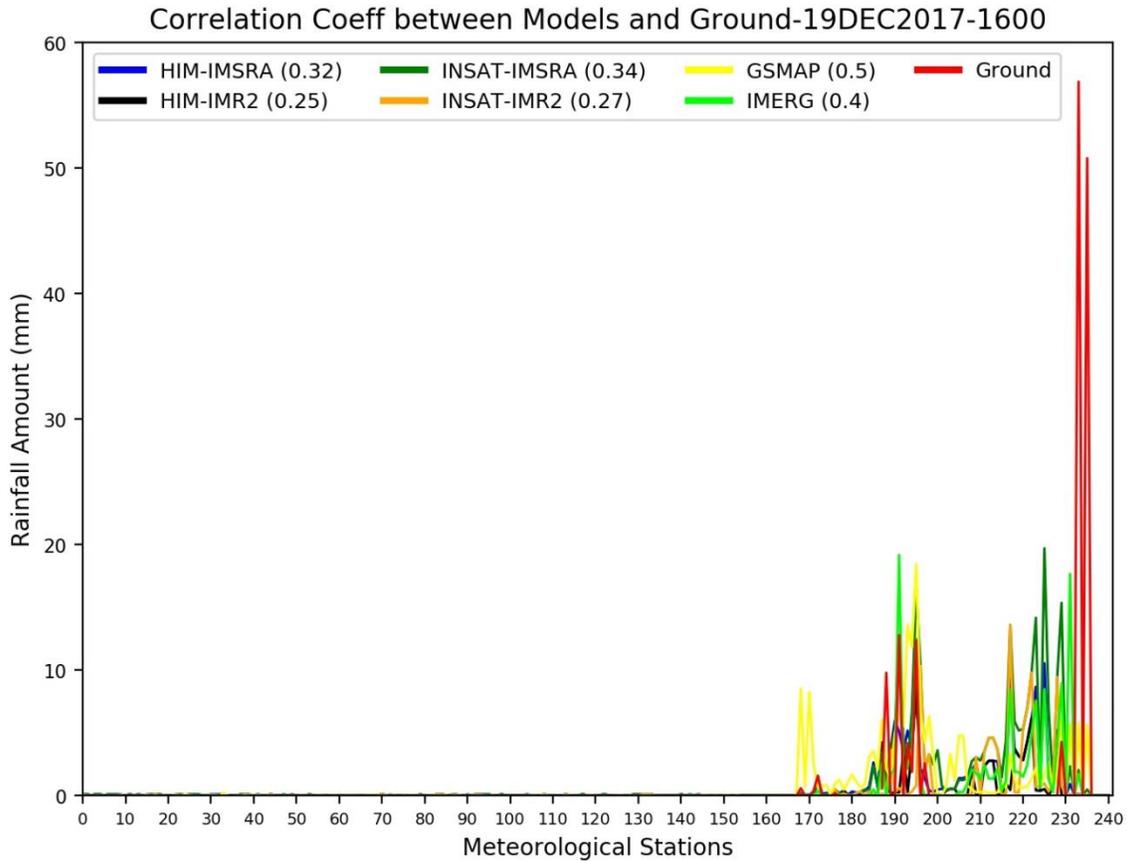
Figure 26. Rainfall distribution at meteorological stations on 19 December 2017 at 1600 UTC

6.0 CONCLUSION

Rainfall estimates by IMSRA and IMR2 have shown some good results using the parameter input of BT-TIR of Himawari satellite, which is as good as the original parameter input by INSAT3D. The rainfall map of the estimates by IMSRA at both Himawari and INSAT3D was observed to be similar to the actual satellite image at each observation. Hence, the rainfall estimates produced by Himawari may be able to provide some now-casting inputs for the observers. Higher correlation coefficient was observed to be about 0.9 between the estimates by IMSRA using BT-TIR from INSAT3D and Himawari but the accuracy was not equally matched with the ground observation. The correlation coefficients between IMSRA for both BT-TIR

Himawari and INSAT3D with ground observation were observed to fall between 0.3 and 0.5 on all observation dates. In general, the result was observed to be the best by IMERG and GSMAP at a correlation of 0.5. Thus, the estimates by BT-TIR from Himawari satellite using the adopted IMSRA estimation model may provide some significant input for the now-casting purposes.

7.0 FUTURE WORK

Although the comparison between the estimates by IMSRA at different BT-TIR from INSAT3D and Himawari showed higher correlation at 0.9, the ground truth validation seems inconsistent among each other. There is a need to develop a rainfall algorithm for the specific Malaysian region to improve the now-casting technique. The brightness temperature of TIR (BT-TIR) from Himawari satellite of the same observation dates of 20 January 2017, 13 July 2017, 04 November 2017 and 19 December 2017 will be collocated and compared points to points with the estimates through the Dual-Frequency Precipitation Radar (DPR) of GPM when the satellite by-passes the region. The regression between the mean Precipitation Radar (PR) derived rainfall rate and Himawari BT-TIR will be calculated. The equation representing the regression will be used as a new rainfall algorithm to match both the local weather and the climate.

ACKNOWLEDGEMENT

REFERENCES

Adler, R.F., Huffman, G.J., Chang, A., Ferraro,R., Xie, P.,Janowiak,J.,(2003). The Version 2 Global Precipitation Climatology Project (GPCP) monthly precipitation analysis (1979-Present). *Journal Hydrometeorology*, 4. 1147-1167.

Bushair, M.T., and R.M. Gairola (2013). Evaluation of KALPANA-1 based rainfall estimation during very severe cyclonic event. SAC/EPSA/AOSG/GRD/SR/04/2013.

Gairola, R. M., A. K. Varma, S. Pokhrel and V. K. Agarwal (2004). Integrated satellite microwave and infrared measurements of precipitation during a Bay of Bengal cyclone, *Indian Journal of Radio and Space Physics*, 33, 115-124.

Gairola, R.M., S. Prakash, and P.K. Pal (2015). Improved rainfall estimation over Indian monsoon region by synergistic use of Kalpana-1 and rain gauge data. *Atmosphere*, 28(1), 51-61.

Gairola, R. M., Anoop Mishra, Satya Prakash and C. Mahesh (2010). Development of INSAT Multispectral Rainfall Algorithm (IMSRA) for monitoring rainfall events over India using KALPANA-IR and TRMM-Precipitation Radar Observations, SAC/EPSA/AOSG/INSAT/SR-39/2010.

Huffman, G. J., R. F. Adler, D. T. Bolvin, G. Gu, E. J. Nelkin, K. P. Bowman, Y. Hong, E. F. Stocker, and D. B. Wolf (2007), The TRMM Multisatellite Precipitation Analysis (TMPA): Quasi-global, multiyear, combined-sensor precipitation estimates at fine scales, *J. Hydrometeorol.*, 8,38-55.

Kubota T., S. Shige, H. Hashizume, A. Aonashi, N. Takahashi, S. Seto, M. Hirose, Y.N. Takayabu, T. Ushio, K. Nakagawa, K. Iwanami, M. Kachi and K. Okamoto (2007). Global precipitation map using satellite-borne microwave radiometers by the GSMaP project: Production and validation. IEE T. *Geosci. Remote*, 45, 2259-2275.

Mishra, A., Gairola, R.M., Varma, A.K., and Agarwal, V.K., (2010). Remote sensing of precipitation over Indian land and oceanic regions by synergistic use of multi-satellite sensors. *Journal of Geophysical Research*, 115, D08106 doi:10.1029/2009JD012157.

Prakash S., C. Mahesh, R.M. Gairola and P.K. Pal (2010). Estimation of Indian summer monsoon rainfall using Kalpana-1 VHRR data and its validation using rain gauge and GPCP data. *Meteorol. Atmos. Phys.* 110, 45-47.

Shaari, N. A. and Gairola , R. M., (2018), Rainfall Assessment for Northeast Monsoon 2015 and 2016 in Malaysia Using INSAT Multispectral Rainfall Algorithm (IMSRA) Technique*, Master Project: Space Application Center (SAC), Indian Space Research Organization (ISRO)*, Ahmedabad, India.